Growth of surfaces generated by a probabilistic cellular automaton

Pratip Bhattacharyya *

Low Temperature Physics Division
Saha Institute of Nuclear Physics
Sector - 1, Block - AF, Bidhannagar
Calcutta 700 064, India.

Abstract

A one-dimensional cellular automaton with a probabilistic evolution rule can generate stochastic surface growth in $(1 + 1)$ dimensions. Two such discrete models of surface growth are constructed from a probabilistic cellular automaton which is known to show a transition from a active phase to a absorbing phase at a critical probability associated with two particular components of the evolution rule. In one of these models, called model A in this paper, the surface growth is defined in terms of the evolving front of the cellular automaton on the space-time plane. In the other model, called model B, surface growth takes place by a solid-on-solid deposition process controlled by the cellular automaton configurations that appear in successive time-steps. Both the models show a depinning transition at the critical point of the generating cellular automaton. In addition, model B shows a kinetic roughening transition at this point. The characteristics of the surface width in these models are derived by scaling arguments from the critical properties of the generating cellular automaton and by Monte Carlo simulations.

*E-mail : pratip@cmp.saha.ernet.in

1 Introduction

Cellular automata are discrete mathematical systems that follow non-equilibrium dynamics [1]. Typically a discrete variable with a finite number of possible states evolves in discrete time-steps, simultaneously at all points of a discrete space (for example, a lattice) on which it has been defined, following a local evolution rule. The simplest of these forms, known as elementary cellular automata, have two states per site and only nearest-neighbour interactions. The evolution of a d-dimensional cellular automaton is by itself a process of surface growth in $(d+1)$-dimensions. Besides, it can generate other surface growth models, for example, by considering the configurations of a cellular automaton in successive time-steps as sieves with pores at the sites that have a particular state and through these pores particles are deposited on the corresponding sites of a substrate lattice.

A cellular automaton with a probabilistic evolution rule will generate a stochastic growth process. When the noise due to the probability is of a non-thermal kind it may bring about a phase transition even in a one-dimensional system with short range interactions [2]. Such a phase transition in a cellular automaton will induce a corresponding effect in the surface growth models generated from it. Generally two kinds of phase transitions are observed in surface growth models : (1) morphological transitions such as kinetic roughening transitions, and (2) depinning transitions. While morphological transitions are due to a critical change in the rate of growth or deposition, depinning transitions occur by a critical increase in the force that drives the surface so that it overcomes the pinning force [3]. Examples of such transitions in $(1+1)$-dimensions are few, most of which are related to a Directed Percolation process : kinetic roughening transitions in $(1+1)$-dimensions have been observed in models of polynuclear growth [4], growth by absorption and desorption of solid on solid [5] and fungal growth [6] whereas depinning transitions in $(1+1)$-dimensions were originally observed in models of quenched point disorder [7] and porous media [8].

This paper reports a study of surface growth phenomena generated by a one-dimensional probabilistic cellular automaton that shows a phase transition in the universality class of Directed Percolation.

2 Two models with depinning transition

The one-dimensional probabilistic cellular automaton (PCA), which is the generator of two surface growth models studied in this paper, is defined as a line of sites with a binary variable $a_i \in \{0, 1\}$ assigned to each site i. A site is said to be occupied if $a_i = 1$ and unoccupied otherwise. The automaton evolves from any given initial configuration $\{a_i^{(0)}\}$ by updating the variables at all lattice sites simultaneously at each time-step. Each site follows a local rule of evolution that involves only nearest-neighbour interactions. The rule is specified by a set of eight components $[a_{i-1}^{(t)}, a_i^{(t)}, a_{i+1}^{(t)}] \mapsto a_i^{(t+1)}$ corresponding to the 2^3 distinct three-site neighbourhoods of interaction :

$$\begin{array}{c|ccccccccc} t: & \underline{111} & \underline{110} & \underline{011} & \underline{101} & \underline{010} & \multicolumn{2}{c}{\underline{100} \quad \underline{001}} & \underline{000} \\ \hline t+1: & 0 & 0 & 0 & 0 & 1 & \multicolumn{2}{c}{\begin{array}{ll} 1 & \text{with probability } p \\ 0 & \text{with probability } 1-p \end{array}} & 0 \end{array} \qquad (1)$$

The probabilistic behaviour enters the cellular automaton as a non-thermal noise added specifically to two mutually symmetric rule components.

Based on the evolution of this PCA from disordered (uncorrelated) initial states two different models of surface growth in $(1 + 1)$ dimensions are constructed :

(1) Model A – The initial configuration of the PCA forms the substrate with the occupied lattice sites acting as growth centers. The propagating front of occupied sites on the space-time plane defines a surface. Here growth occurs in the direction of increasing time which therefore is the vertical direction along which the surface height will be measured. Overhangs may exist on the front but they are ignored so that the height profile is a single-valued function. The height of the surface $h_i(t)$ above a point i on the substrate at time t is given by the time coordinate of the highest occupied site in the i-th column which means that in this model all sites in a column in the space-time plane between the substrate site and the highest occupied site are assumed to be filled. This is a growth model of the propagating interface type.

(2) Model B – This is a model of the deposition type. Surface growth takes place on a one-dimensional substrate (a line of empty sites) by depositing particles in successive time-steps

according to the configuration of the cellular automaton at those times. At time t a particle is added to the i-th column, i.e., the height of the i-th column is increased by unity if the corresponding site in the PCA is occupied at that time ($a_i^{(t)} = 1$). The height variable is defined by :

$$h_i(t) = \sum_{\tau=1}^{t} a_i^{(\tau)} \, . \tag{2}$$

A surface grown in this way does not have overhangs. Figure 1 shows typical examples of surfaces of models A and B generated by the evolving cellular automaton. To illustrate the procedure of growth in the two models outlined above the detailed mechanics are shown schematically for a small part of the lattice.

The purpose of having disordered initial states of the PCA is to avoid the appearance of absorbing states at the beginning of its evolution. The PCA is known to have three absorbing states [10] : the zero configuration ($\cdots 0000 \cdots$) and two mutually symmetric configurations given by sequences of alternating 0 and 1 ($\cdots 0101 \cdots$, $\cdots 1010 \cdots$). Occurence of these absorbing states leads to either no growth (for the zero configuration) or a trivial growth process (for the other two absorbing states). A disordered state is constructed by assigning each lattice site the value 1 with a predefined probability and 0 otherwise, independently of the values at other lattice sites; when this probability is $\frac{1}{2}$ the state is said to be completely random. In general, any initial state other than the three absorbing states will serve this purpose.

The growth models are characterised by the properties of their surface width which, for a substrate of linear size L, is defined in the usual way [3] :

$$w^2(L,t) = \left\langle \, \overline{\left[h_i(t) - \bar{h}(t) \right]^2} \, \right\rangle \, , \tag{3}$$

$\bar{h}(t) = \frac{1}{L} \sum_{i=1}^{L} h_i(t)$ is the average height of the surface above the substrate at time t. The bar $\overline{\cdots}$ denotes average over the system and the angular brackets $\langle \cdots \rangle$ denote configurational average. In the addition to the width, a moving surface is characterised by its average velocity of propagation, defined by [3] :

$$v_t = \frac{\partial}{\partial t} \bar{h}(t) \, . \tag{4}$$

For the PCA model there exists a critical value of p, observed to be $p_c \approx 0.75$ [9], at which a continuous phase transition occurs with respect to the density of occupied sites in the steady

state; Monte Carlo simulations [10] of the PCA indicate that the phase transition belongs to the universality class of Directed Percolation. In the absorbing phase ($p < p_c$) all initial configurations other than the two mutually symmetric absorbing states following the rule in equation (1) evolve to the zero configuration (all sites unoccupied) which is a absorbing state of the PCA. Evolution of the cellular automaton stops when the zero configuration is reached. The presence of occupied sites in the cellular automaton configuration at any time-step produces a moving surface in the growth models. The appearance of the zero configuration results in pinning of the surface [1]. In the active phase ($p > p_c$) all initial configurations other than the three absorbing states evolve to a active steady state with a non-zero density of occupied sites. This results in unpinned surfaces in the growth models.

Thus the critical point p_c of the cellular automaton marks a depinning transition in the growth models, from a pinned phase for $p < p_c$ to a moving phase for $p > p_c$. The order parameter for the phase transition in the cellular automaton is the density of occupied sites ρ_∞ in the steady state which in the supercritical region decreases continuously to zero as the critical point is approached [9] :

$$\rho_\infty \propto (p - p_c)^\beta, \qquad p \to {p_c}^+ . \tag{5}$$

The appropriate order parameter in the growth models in general is the asymptotic velocity v_∞ of the surface in the moving phase [3] :

$$v_\infty \propto (p - p_c)^\theta, \qquad p \to {p_c}^+ . \tag{6}$$

The following sections report the investigations on the depinning transition in models A and B by scaling arguments and Monte-Carlo simulations.

3 Properties of Model A

By definition Model A is the direct evolution of the PCA from disordered initial states viewed as a growth process that excludes surface overhangs. Therefore the properties of the surface near the depinning transition can be derived from those of the critical properties of the PCA. Figure 2(a,b) shows typical examples of evolution of the surface width $w(L, t)$

[1] Though pinning centers and forces are not explicit in these models, pinning of a surface growing in $(d+1)$-dimensions can be thought of as a d-dimensional system entering an absorbing state where there are no particles.

with time for substrates of different sizes L obtained by Monte Carlo simulation of Model A. As it is usual for correlated growth on substrates of finite size the surface width gets saturated after a crossover time $t_\times$. Both above and below the depinning transition point p_c the saturated value of the width, denoted by $w(L,\infty)$, shows two regimes separated by a crossover length $L_\times$ – (1) for $L \ll L_\times$ it increases with L indicating the appearance of a 'rough' (or, L-dependent) regime; (2) for $L \gg L_\times$, $w(L,\infty)$ tends to saturate to a constant value as $L \to \infty$ which indicates a 'smooth' (or, L-independent) regime. The values of $L_\times$ and $w(\infty,\infty)$ depend only on the value of the noise parameter p. Therefore the saturated width $w(L,\infty)$ is expected to follow a scaling relation of the form

$$\frac{w(L,\infty)}{w(\infty,\infty)} \propto f_{<>}\left(\frac{L}{L_\times}\right), \tag{7}$$

where $f_<$, $f_>$ denotes the scaling function in the pinned ($p < p_c$) and moving ($p > p_c$) phases respectively.

The crossover length $L_\times$ provides a characteristic lengthscale of the model. Because of the scaling hypothesis that the model has a unique diverging lengthscale at the critical point, $L_\times$ must diverge as the correlation length of the PCA as p approaches p_c from above and below :

$$L_\times \propto |p - p_c|^{-\nu_\perp}, \tag{8}$$

where $\nu_\perp$ is the critical exponent for the correlation length of the PCA. Since the growth of the surface occurs in the direction of time, the saturated surface width is a measure of temporal RMS fluctuations in the steady state. Consequently, in the limit of an infinite substrate, the quantity $w(\infty,\infty)$ will diverge as the correlation time of the PCA :

$$w(\infty,\infty) \propto |p - p_c|^{-\nu_\parallel}, \tag{9}$$

This reduces the scaling law (7) to the standard form of finite size scaling [11] :

$$w(L,\infty)\,|p - p_c|^{\nu_\parallel} \propto f_{<>}(L\,|p - p_c|^{\nu_\perp}). \tag{10}$$

Since the PCA is believed to be in the universality class of Directed Percolation [10], the critical exponents for $L_\times$ and $w(\infty,\infty)$ are expected to be $\nu_\perp = \nu_\perp^{DP} \approx 1.097$ and $\nu_\parallel = \nu_\parallel^{DP} \approx 1.734$ respectively [12].

At p_c the crossover length $L_\times$ diverges and only the rough regime exists. The surface width is then expected to follow the Family-Vicsek scaling law [13] :

$$w(L,t) \propto L^\alpha f\left(\frac{t}{L^z}\right), \qquad p = p_c\,. \tag{11}$$

The growth exponent λ and the roughness exponent α are defined as $w(L,t) \propto t^\lambda$, $t \ll t_\times$ and $w(L,t) \propto L^\alpha$, $t \gg t_\times$ respectively and the dynamic exponent z occuring in (11) is given by $t_\times \propto L^z$, $z = \alpha/\lambda$. The value of the exponents α, λ and z at p_c can be obtained by using the scaling hypothesis : corresponding to a uniquely diverging lengthscale of the model there exists a uniquely diverging timescale. The saturated width $w(L,\infty)$ in this model measures temporal RMS fluctuations in the steady state and in the thermodynamic limit ($L \to \infty$) it must diverge as the correlation time as p approaches p_c. For a finite-sized system (substrate) at $p = p_c$, $w(L,\infty) \propto L^{\nu_\parallel/\nu_\perp}$ which gives the roughness exponent :

$$\alpha_{p=p_c} = \frac{\nu_\parallel}{\nu_\perp}\,. \tag{12}$$

Similarly the crossover time $t_\times$ is another way of defining the characteristic timescale for the model and shall have the form $t_\times \propto L^{\nu_\parallel/\nu_\perp}$ at $p = p_c$. Therefore the dynamic exponent is given by :

$$z = \frac{\nu_\parallel}{\nu_\perp}\,. \tag{13}$$

Since the phase transition of PCA is believed to be in the universality class of Directed Percolation [10],

$$\alpha_{p=p_c} = z = \frac{\nu_\parallel^{DP}}{\nu_\perp^{DP}} \approx 1.58\,. \tag{14}$$

Therefore the growth exponent at $p = p_c$ becomes equal to unity :

$$\lambda_{p=p_c} = \frac{\alpha_{p=p_c}}{z} = 1\,. \tag{15}$$

To confirm the results obtained above from scaling considerations Monte Carlo simulations of the growth process in Model A were performed on substrates of sizes $L = 100$ to $L = 10000$. A disordered substrate is constructed by assigning to each lattice site the value 1 with probability $\frac{1}{2}$ and 0 otherwise. For each substrate size 2000 independent simulations were done for the purpose of averaging out statistical fluctuations.

Figure 3 shows the results of applying scaling relation (10) to the simulation data for the surface width. Data for $w(L,\infty)$ *vs* L in the pinned phase, for different values of p close to p_c, collapse to a single curve for the following values of the transition point and the critical exponents :

$$p_c = 0.7513 \pm 0.0004\,; \tag{16}$$

$$\nu_\perp = 1.1 \pm 0.01\,, \qquad \nu_\parallel = 1.73 \pm 0.01\,. \tag{17}$$

Similarly for the moving phase, values of the critical point and exponents were obtained by collapsing the simulation data for $w(L,\infty)$ *vs* L for different values of p close to p_c :

$$p_c = 0.7511 \pm 0.0004\,; \tag{18}$$

$$\nu_\perp = 1.1 \pm 0.01\,, \qquad \nu_\parallel = 1.74 \pm 0.01\,, \tag{19}$$

These are found to agree, within the limits of error, with the corresponding values for the pinned phase. Error bars indicated here and elsewhere in the paper are statistical errors.

The estimate of the depinning transition point p_c obtained here agrees well with the value of the critical point of the PCA measured by using defect dynamics [10]. The estimates of the critical exponents are in good agreement with the values for the universality class of Directed Percolation [12].

To measure the surface exponents for $p = p_c$ simulations were performed at $p = 0.7512$. The time taken for the PCA to reach a steady state is very large and the width of the surface could not be measured till saturation. Therefore a direct determination of α and z at p_c was not possible with the available computer facility. However the surface width (averaged over 5000 intial configurations) was observed to grow linearly on a substrate of size $L = 10^4$ for 10^5 times-steps (Figure 4), thus establishing $\lambda_{p=p_c} = 1$ and $\alpha_{p=p_c} = z$, in agreement with equation (15). Analyses of simulation data far from p_c show that the 'rough' regime occurs for only very small system sizes ($L \ll L_\times$) and the dependence of $w(L,\infty)$ on L is logarithmic for the most part of the crossover region. The 'rough' regime grows as p approaches p_c and $w(L,\infty)$ becomes entirely a power-function of L at $p = p_c$. Thus a true 'rough' surface (in the sense of $\alpha > 0$) exists only at the transition point.

The last result of this section is concerned with the velocity of the surface in the moving phase. Simulations of the growth process A for different values of p show that the surface in the moving phase attains the maximum velocity asymptotically, $v_\infty = 1$, irrespective of the value of p (Figure 5). Consequently v_∞ cannot serve as the order parameter for the depinning transition in Model A. The appropriate order parameter is the asymptotic density of columns with the maximum height which is equal to the density of occupied sites in the steady state of the generating PCA and hence it decays by the power-law (5) with the critical exponent $\beta = \beta^{DP} \approx 0.276$.

4 Properties of Model B

Model B defines a deposition process of the solid-on-solid type, i.e., the bulk of the aggregate is compact (no vacancies) and there are no surface overhangs. Consider first the moving phase ($p > p_c$). Since there is no interaction between the columns of the aggregate, correlations do not develop along its surface; hence the surface width in the moving phase does not saturate. When the PCA evolves from a disordered initial state the process can be described by a continuum equation similar to the one describing a ordinary random deposition process [3] :

$$\frac{\partial}{\partial t} h(x,t) = F + \eta(x,t), \tag{20}$$

where F is the average number of particles arriving at a site and η is the noise term (with zero configurational average : $\langle \eta(x,t) \rangle = 0$) that describes the fluctuations in the deposition process. The difference between the random deposition model and this model lies in the noise correlations. While the noise in random deposition is uncorrelated, the spatial and temporal correlations developing in the generating PCA appear as noise correlations in model B. Since the initial state of the PCA is disordered the growth process in the first time-step looks like random deposition. But correlations in space and time develope in the PCA configuration as it evolves owing to the nearest-neighbour interactions defined in the evolution rule (1). For values of p away from p_c, the correlation length ξ and the correlation time τ of the PCA are finite which means the noise in the deposition process is correlated over a short range described by exponential decay of the correlation function [3] :

$$\langle \eta(x,t)\eta(x',t') \rangle \sim e^{-|x-x'|/\xi}\, e^{-|t-t'|/\tau}. \tag{21}$$

The effects of the correlated noise is prominent for times less than τ. Since deposition at time-step $t+1$ is allowed only at or next to sites where deposition has taken place in the previous time-step t [along with the restrictions set by the PCA evolution rule (1)] the height fluctuations about the mean value are larger and hence the growth of the surface width is faster than that for random deposition. For times greater than τ the noise appears uncorrelated and the growth exponent λ will reduce to the random deposition value $\lambda^{RD} = \frac{1}{2}$. As p approaches p_c, ξ and τ increase and it takes longer for the growth process to reach the random deposition limit. This is illustrated in Figure 6. Finally, at $p = p_c$, both ξ and τ diverge and the correlations in the noise are long-ranged, represented by a power-law decay of the noise correlation function [3] :

$$\langle \eta(x,t)\eta(x',t') \rangle \sim |x-x'|^{-2\beta/\nu_\perp} \, |t-t'|^{-2\beta/\nu_\parallel}. \tag{22}$$

where β, $\nu_\perp$ and $\nu_\parallel$ are the critical exponents for the order parameter, correlation length and correlation time of the PCA respectively. The asymptotic value of the growth exponent λ at p_c can be derived from the continuum equation (20) where $\eta(x,t)$ follows the correlation function (22) instead of the delta-correlated noise of a random deposition process. The surface width for a infinite substrate is found to increase as the following power function of the time :

$$w(\infty,t) \propto t^{1-\beta/\nu_\parallel}. \tag{23}$$

Using the indication that the phase transition in the PCA belongs to the universality class of Directed Percolation [10], the value of the growth exponent at p_c is expected to be :

$$\lambda_{p=p_c} = 1 - \frac{\beta^{DP}}{\nu_\parallel^{DP}} \approx 0.841. \tag{24}$$

At this point the surface grown on a finite substrate enters the pinned phase.

The behaviour of the velocity of the surface in the moving phase can be analysed as follows. The average height of the surface above the substrate at time-step t is equal to the number of particles deposited per site in the interval $[0,t]$ averaged over the entire system. The velocity of propagation v_t of the surface at time-step t, defined by Eq. (4), is therefore equal to the average number of particles deposited per site in the $t-$th time-step. This number is precisely the density of occupied sites ρ_t of the generating PCA at time t :

$$v_t = \rho_t. \tag{25}$$

In the steady state, as p appoaches p_c, the asymptotic velocity v_∞ of the surface will thus decrease to zero by the power-law followed by ρ_∞. This implies, after comparing equations (5) and (6), that $\theta = \beta$. Since the phase transition of the PCA is known to be in the universality class of Directed Percolation [10], the critical velocity exponent is given by :

$$\theta = \beta^{DP} \approx 0.276. \tag{26}$$

The model B in the moving phase was studied numerically by Monte Carlo simulations of the growth process on a one-dimensional lattice of $L = 10^4$ sites for various values of p ($p > p_c$) and results for each value of p were averaged over 10^3 independent realisations of the process obtained by constructing the disordered initial states of the PCA independently of one another. Figure 6(a) shows the surface width as a function of time for different values of p, drawn on double-logarithmic scale. To determine the growth exponent λ an effective exponent λ_t is defined as the local slope of the curves drawn in Figure 6(a) :

$$\lambda_t = \frac{\log[w(L,t)/w(L,t/b)]}{\log b}. \tag{27}$$

With $b = 5$, λ_t was calculated for different values of p upto $t = 10^5$ time-steps and plotted against $1/t$ (Figure 6b). All curves for $p > p_c$ tend to the random deposition value $\lambda^{RD} = \frac{1}{2}$; though the curves for p close to p_c do not reach this value in 10^5 time-steps they clearly show a tendency to do so at a larger t. For $p = 0.7512(\approx p_c)$, in order to remove finite-size effects, the growth exponent was obtained by extrapolating the maximum values of the effective exponent measured for different substrate sizes :

$$\lambda_{p=p_c} \approx \max\left[\lambda_t(p = 0.7512)\right] = 0.837 \pm 0.011, \tag{28}$$

which is close to the expected value for an infinite substrate [equation (24)]. In the curve for $p = 0.7512$ in Figure 6(b) a decrease observed in the value of λ_t after it reaches a maximum is due to the finite size of the substrate used in the simulation and it shows the beginning of a crossover to saturation of the surface width, the system having just entered the pinned phase at p_c.

The asymptotic velocity v_∞ of the surface obtained from the simulation data (Figure 7) show that the power-law behaviour of v_∞ as $p \to p_c^+$ [equation(6)] is best satisfied with :

$$p_c = 0.7514 \pm 0.0004. \tag{29}$$

This independent estimate of p_c agrees well previous estimates [10] and those obtained from the study of model A in this paper. The value of the velocity exponent was measured to be :

$$\theta = 0.274 \pm 0.007, \tag{30}$$

which agrees, within the limits of error, with the expected value given in equation (26).

Consider now the pinned phase. For $p < p_c$ growth of the aggregate stops in finite time (which depends on the parameter p) due to the appearence of the absorbing state of the generating PCA. The time for which growth takes place is equal to the *transient time* T of the generating PCA, i.e., the number of time-steps required by the PCA to evolve from a disordered initial configuration to the absorbing zero configuration. Like that of model A, the surface width $w(L,t)$ saturates after a crossover time $t_\times$ for a substrate of finite size. The behaviour of the saturated width $w(L,\infty)$ too resembles that of model A : after an initial L-dependent regime it passes over to a L-independent regime (Figure 2c) beyond a crossover length $L_\times$. Thus for $p < p_c$ the surface in model B is smooth (in the sense of $\alpha = 0$) in the thermodynamic limit ($L \to \infty$). Only at the depinning transition point p_c, where $L_\times$ diverges, the surface is rough ($\alpha > 0$) for all substrate sizes and the Family- Vicsek law (11) is expected to hold true. Since the saturation of the surface width is forced by the PCA, the crossover time $t_\times$ will be the same as that of model A which means the dynamic exponent at p_c is given by the Directed Percolation value :

$$t_\times(p = p_c) \propto L^z, \qquad z = z^{DP} \approx 1.58. \tag{31}$$

At p_c, just before the surface enters the moving phase, the roughness exponent is given by :

$$\alpha_{p=p_c} = z \cdot \lambda_{p=p_c} = z^{DP}(1 - \beta^{DP}/\nu_\parallel^{DP}) \approx 1.33. \tag{32}$$

This result for α could not be verified by Monte Carlo simulations on available computer facility as it takes enormous times for the surface width on substrates of reasonable sizes to reach saturation at p_c.

Since the surface width does not saturate in the moving phase, it becomes infinitely large with time. Therefore the depinning transition point also marks a kinetic roughening transition from a smooth surface in the pinned phase to a infinitely rough surface in the moving phase.

5 Discussion

In the two models studied in this paper the dynamics of surface growth are derived from the evolution rule of a one-dimensional probabilistic cellular automaton. While model A presents the growth of an aggregate of interacting particles, model B presents the growth of an aggregate of non-interacting particles deposited by a correlated mechanism. This results in the formation of a correlated surface in model A and an uncorrelated surface in model B. The correlated mechanics of deposition in model B leads to growth of the surface width of the aggregate at the depinning transition point p_c with an exponent λ larger than that offered the ordinary random deposition model. This result follows the trend that the growth exponent increases in the presence of correlations in the deposition process, observed previously in ballistic deposition models [14]. Also the surface properties of the models at the depinning transition are all related to the critical properties of the generating PCA. It is yet to be seen the effect of introducing in these models the additional dynamics of surface restructuring.

Finally, a comment on the scaling relation [3] :

$$\theta = (z - \alpha)\nu, \tag{33}$$

which relates the exponents for roughness, growth and velocity of the surface to the exponent ν for the correlation length along the surface at a depinning transition. For model A at p_c, $\nu = \nu_\perp$ and $\alpha = z$ so that $\theta = 0$; this is true as the velocity in the moving phase is independent of the level of noise p which provides the driving force. For model B at p_c, the values of θ, z and α from equations (26), (31) and (32) give $\nu = \nu_\perp$; this is not true. Since there is no inter-columnar interaction at the surface of the aggregate, correlations do not develop along the surface and an exponent ν cannot be associated with it; the scaling relation (33) therefore does not hold in this case.

Acknowledgement

I am grateful to Bikas K. Chakrabarti for his critical comments on the work. A part of this work was supported by CSIR, Government of India.

References

[1] S. Wolfram, Rev. Mod. Phys. **55**, 601 (1983).

[2] P. Grassberger, F. Krause, T. von der Twer, J. Phys. A: Math. Gen. **17**, L105 (1984).

[3] A-L. Barabasi, H. E. Stanley, in *Fractal Concepts in Surface Growth* (Cambridge University Press, Cambridge 1995).

[4] J. Kertesz, D. E. Wolf, Phys. Rev. Lett. **62**, 2571 (1998).

[5] U. Alon, M. R. Evans, H. Hinrichsen, D. Mukamel, Phys. Rev. Lett. **76**, 2746 (1996); Phys. Rev. E **57**, 4997 (1998).

[6] J. M. Lopez, H. J. Jensen, Phys. Rev. Lett. **81**, 1734 (1998).

[7] L-H. Tang, H. Leschhorn, Phys. Rev. A **45**, R8309 (1992).

[8] S. Buldyrev, A-L. Barabasi, F. Caserta, S. Havlin, H. E. Stanley, T. Vicsek, Phys. Rev. A **45**, R8313 (1992).

[9] P. Bhattacharyya, Physica A **234**, 427 (1996).

[10] P. Bhattacharyya, Eur. Phys. J. B **3**, 247 (1998).

[11] M. N. Barber, 'Finite-size Scaling', in *Phase Transitions and Critical Phenomena*, vol. 8, edited by C. Domb, J. L. Lebowitz (Academic Press, London 1983).

[12] I. Jensen, J. Phys. A: Math. Gen. **29**, 7013 (1996).

[13] F. Family, T. Vicsek, J. Phys. A: Math. Gen. **18**, L75 (1985).

[14] P. Meakin, R. Jullien, Europhys. Lett. **9**, 71 (1989); Phys. Rev. A **41**, 983 (1990).

Figure Captions

Figure 1. (a) An example of the evolution of the probabilistic cellular automaton following the rule in equation (1) for $p = 0.8$. Sites (i, t) on the space-time plane with automaton value $a_i^{(t)} = 1$ are marked dark while those with automaton value $a_i^{(t)} = 0$ are left blank. (b) The surface of model A and (c) that of model B at the 250-th time-step of the automaton evolution shown in (a). (d) Schematic diagram showing the construction of the surfaces of models A and B : model A is constructed from the PCA pattern by filling all vacant sites below the highest occupied site in every column whereas model B is constructed by considering the occupied sites in the PCA pattern as particles and dropping them one above the other in a ordered way in every column. The surfaces are shown by lines joining the highest point in each column.

Figure 2. The development of the surface width in time on substrates of different sizes : (a) model A in the pinned phase ($p = 0.7$), (b) model A in the moving phase ($p = 0.8$), (c) model B in the pinned phase ($p = 0.73$).

Figure 3. Data collapse obtained by applying the finite-size scaling relation in equation (10) to the simulation data for the saturated surface width of model A in the (a) pinned and (b) moving phases.

Figure 4. The growth of the surface width of model A at the depinning transition point $p_c \approx 0.7512$. The solid line shows the result of simulation on a lattice of 10^4 sites; the dashed line represents a linear growth of the surface width : $w(L, t) \propto t$. At large times the surface width is seen to grow linearly with time as it becomes parallel to the dashed line.

Figure 5. The average velocity of the surface, defined by equation (4), in the moving phase of model A is plotted against time. For all values of p, a few of which are shown here, the velocity asymptotically attains the maximum possible value of one lattice constant per time-step.

Figure 6. (a) The growth of the surface width of model B in time for different values of p in the moving phase. Simulation data are shown for the following values of p : 0.7512 (top), 0.754, 0.756, 0.758, 0.76, 0.77, 0.78, 0.79, 0.8 and 0.9 (bottom). The curves do not appear to saturate even after 10^5 time-steps of evolution, which agrees with the

theory. (b) The effective growth exponents λ_t derived as local slopes of the curves shown in (a). The curves for $p = 0.754, \ \ldots \ , 0.9$ tend to the random deposition value $\lambda = 0.5$ as $t \to \infty$. The downward bending of the curve for $p = 0.7512$ is a signature of relaxation toward a saturated state; this is not easily evident from the corresponding curve in (a).

Figure 7. The asymptotic velocity of model B in the moving phase for different values p near p_c. The inset shows that it decreases to zero by a power-law as p approaches p_c. The slope of the dashed line gives the value of the velocity exponent θ (see text).

Figure 1(a)

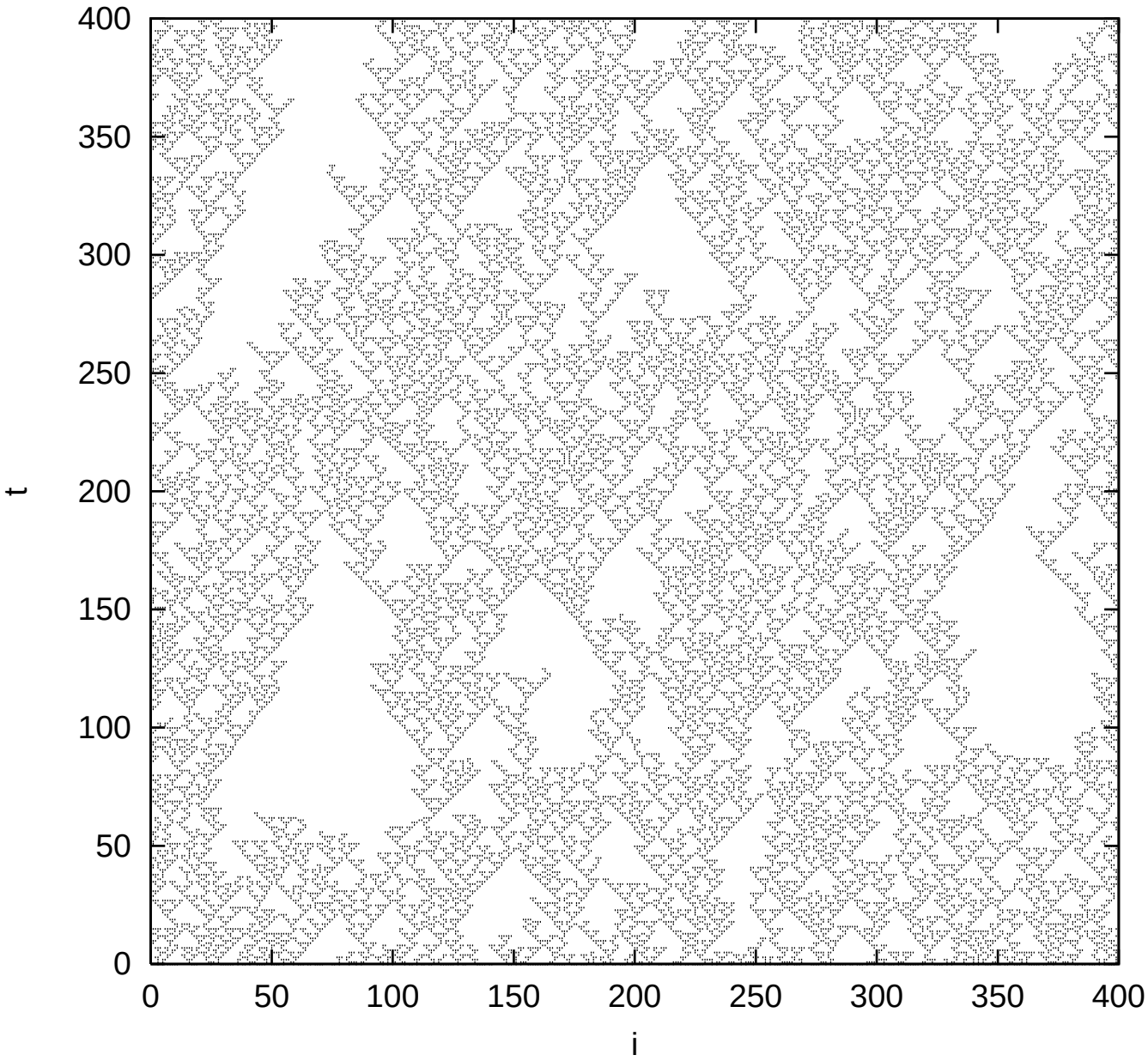
400
350
300
250
200
150
100
50
0
t
0
50
100
150
200
250
300
350
400
i

Figure 1(b)

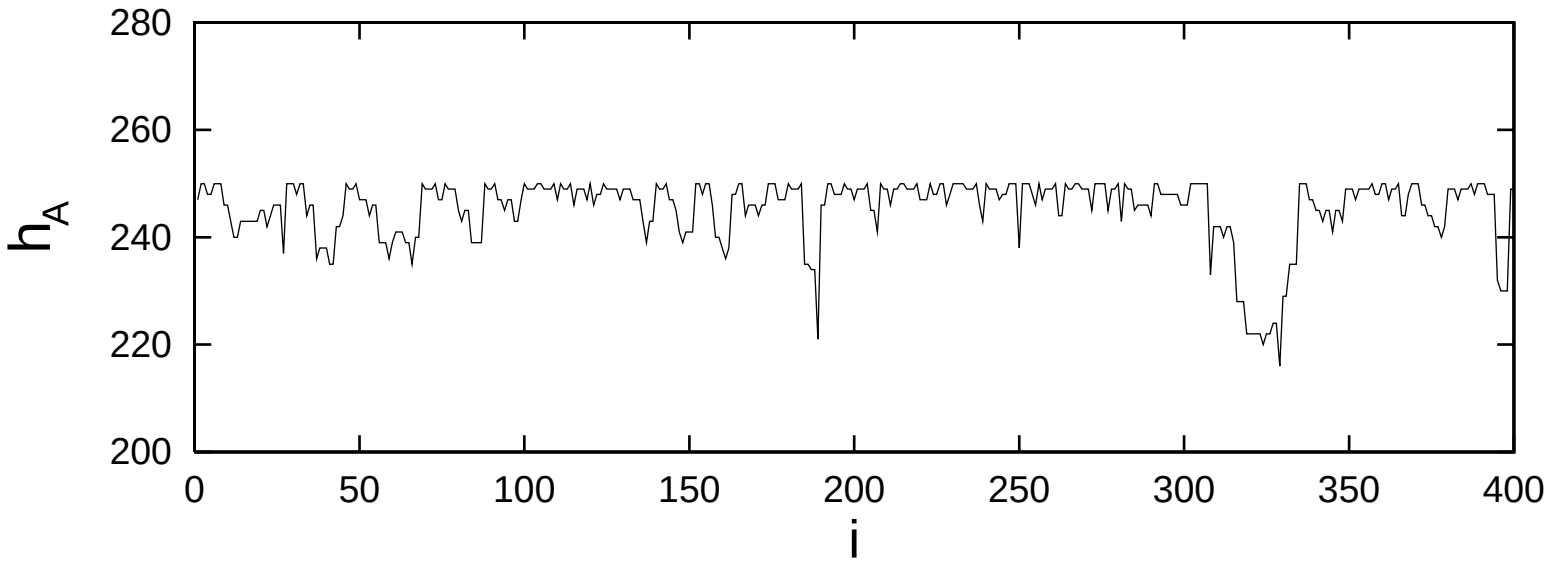

Figure 1(c)

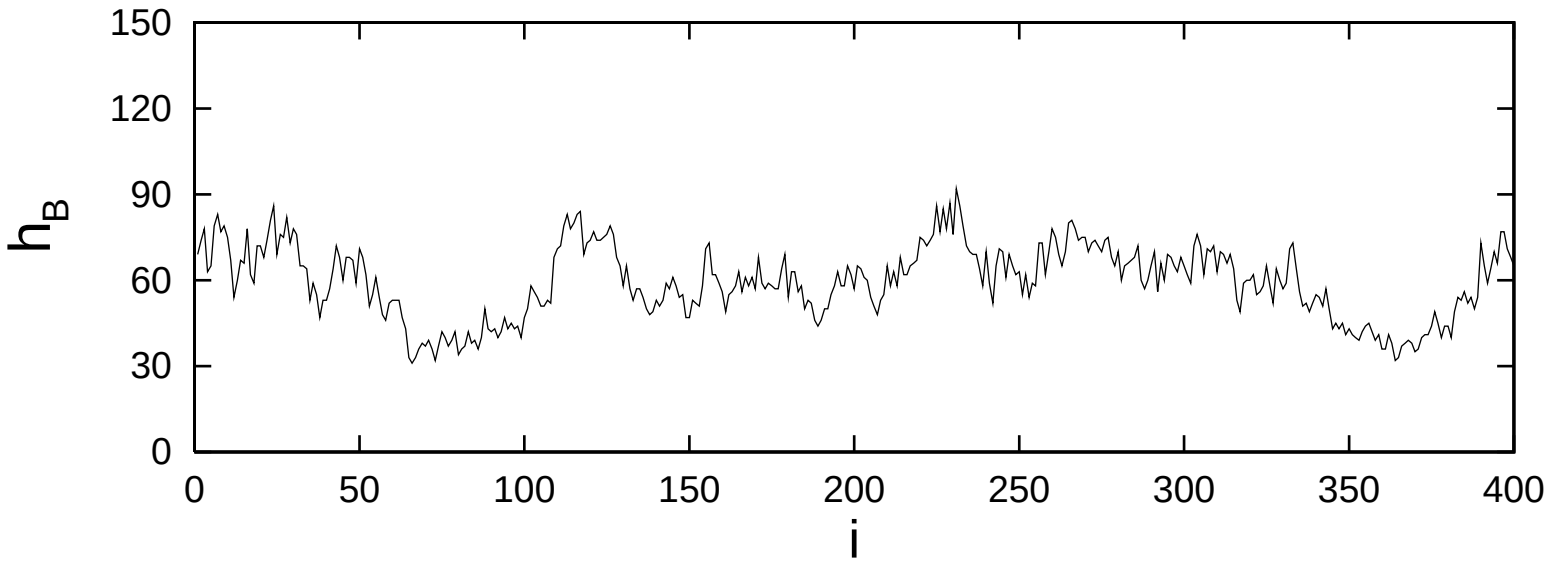

Figure 1(d)

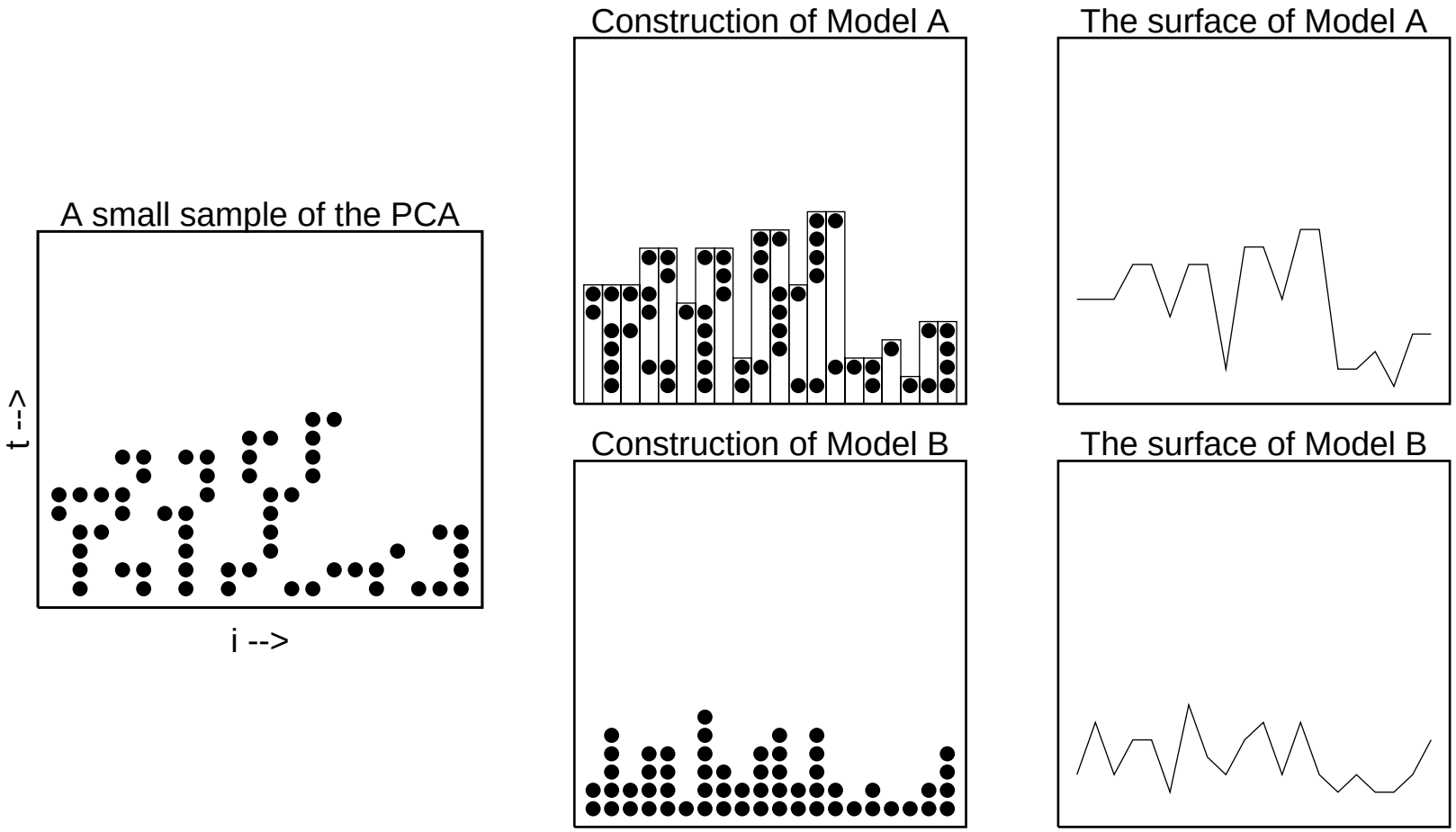
A small sample of the PCA
t -->
i -->
Construction of Model A
The surface of Model A
Construction of Model B
The surface of Model B

Figure 2(a)

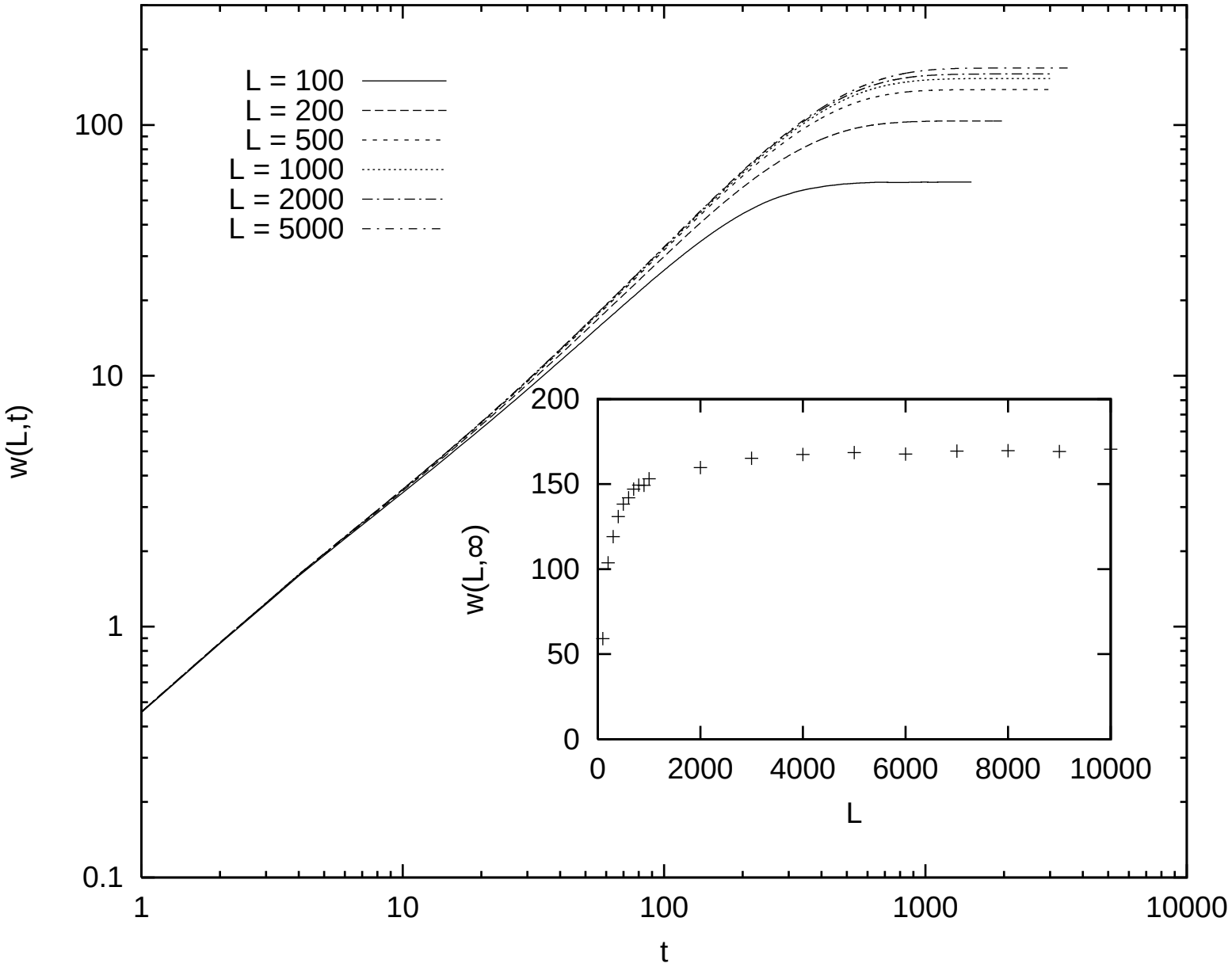
L = 100
L = 200
L = 500
L = 1000
L = 2000
L = 5000
w(L,t)
t
100
10
1
0.1
1
10
100
1000
10000
w(L,∞)
L
200
150
100
50
0
0
2000
4000
6000
8000
10000

Figure 2(b)

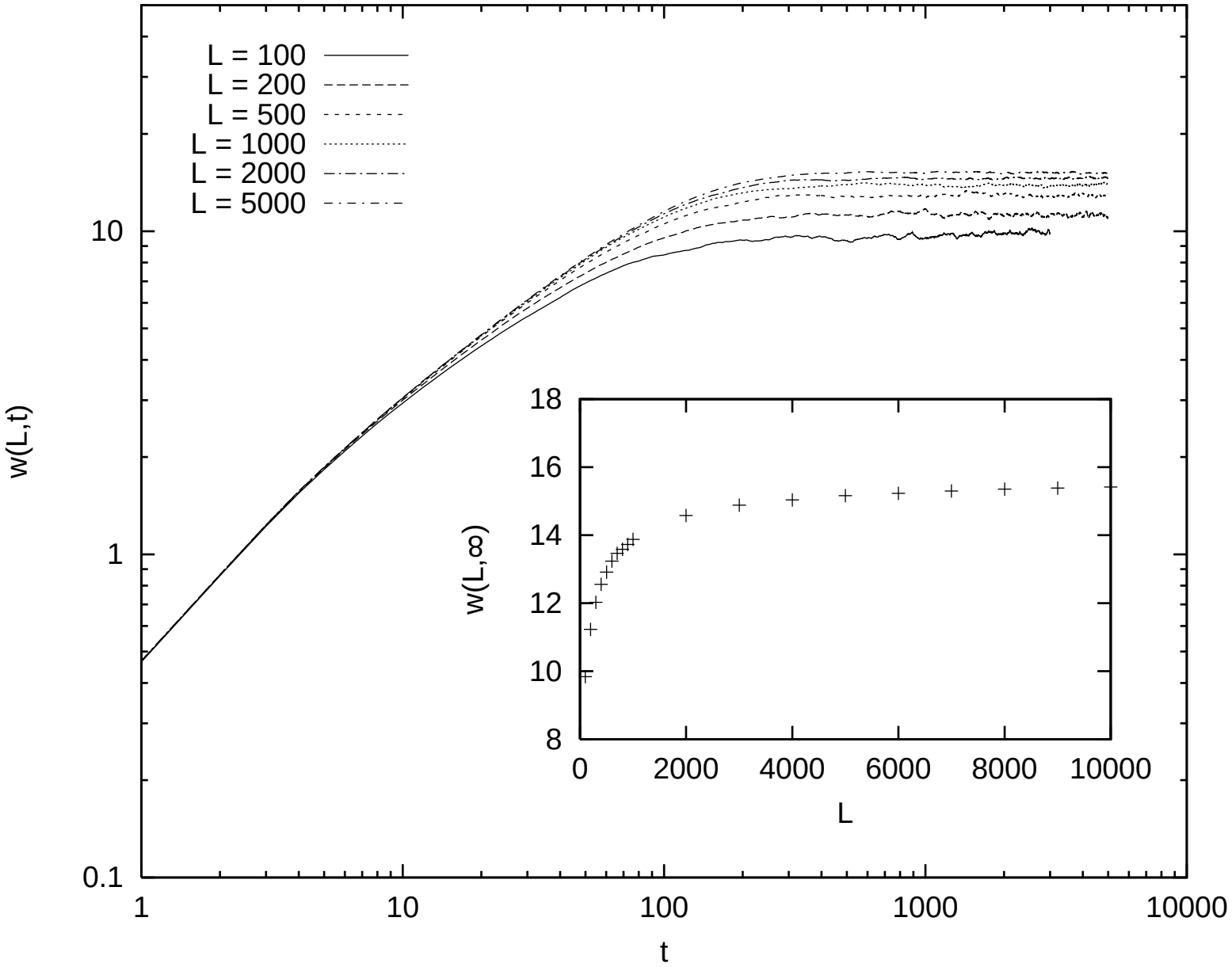
L = 100
L = 200
L = 500
L = 1000
L = 2000
L = 5000
w(L,t)
t
0.1
1
10
1
10
100
1000
10000
w(L,∞)
L
8
10
12
14
16
18
0
2000
4000
6000
8000
10000

Figure 2(c)

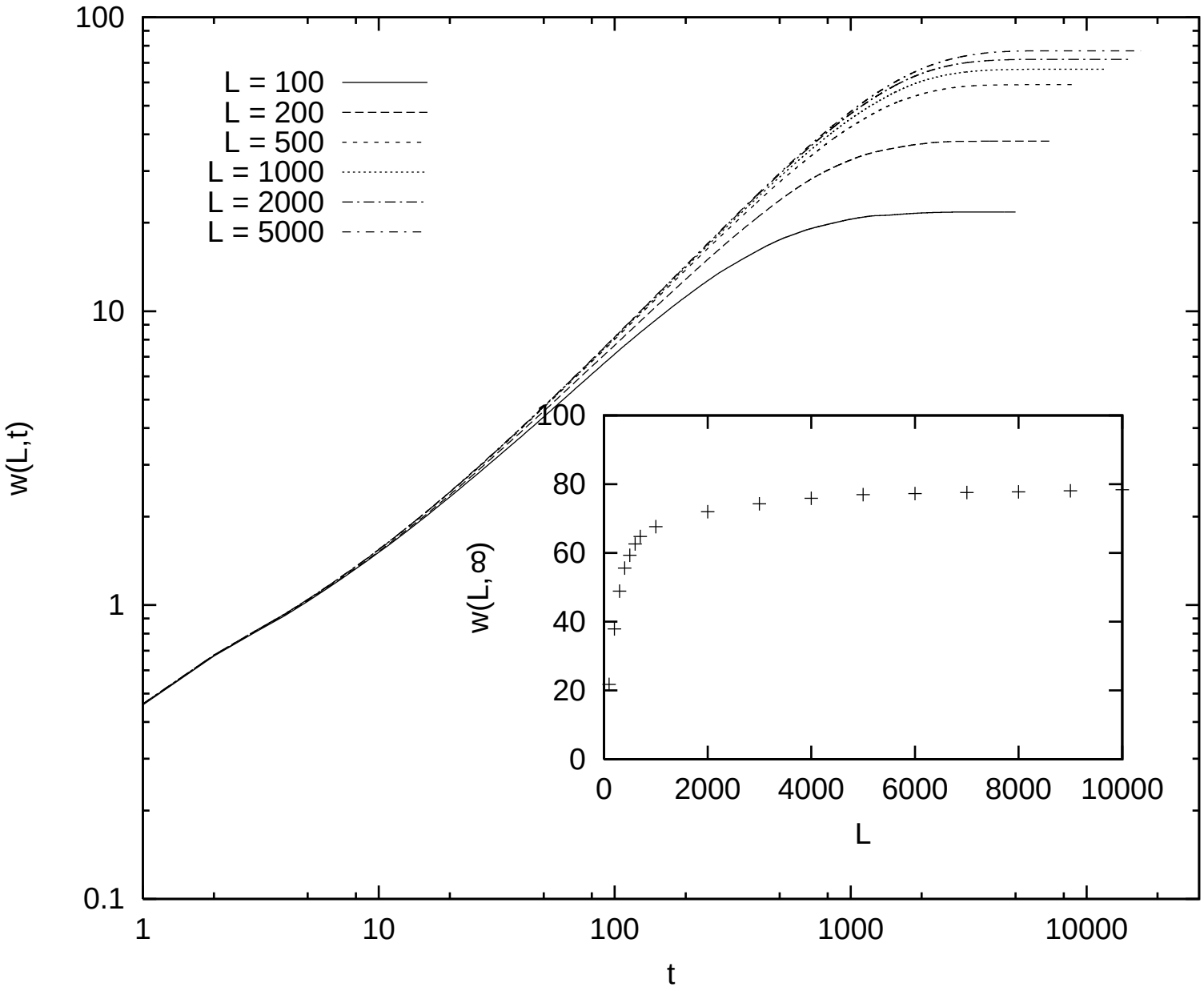
100
10
1
0.1
w(L,t)
1
10
100
1000
10000
t
L = 100
L = 200
L = 500
L = 1000
L = 2000
L = 5000
w(L,∞)
100
80
60
40
20
0
0
2000
4000
6000
8000
10000
L

Figure 3(a)

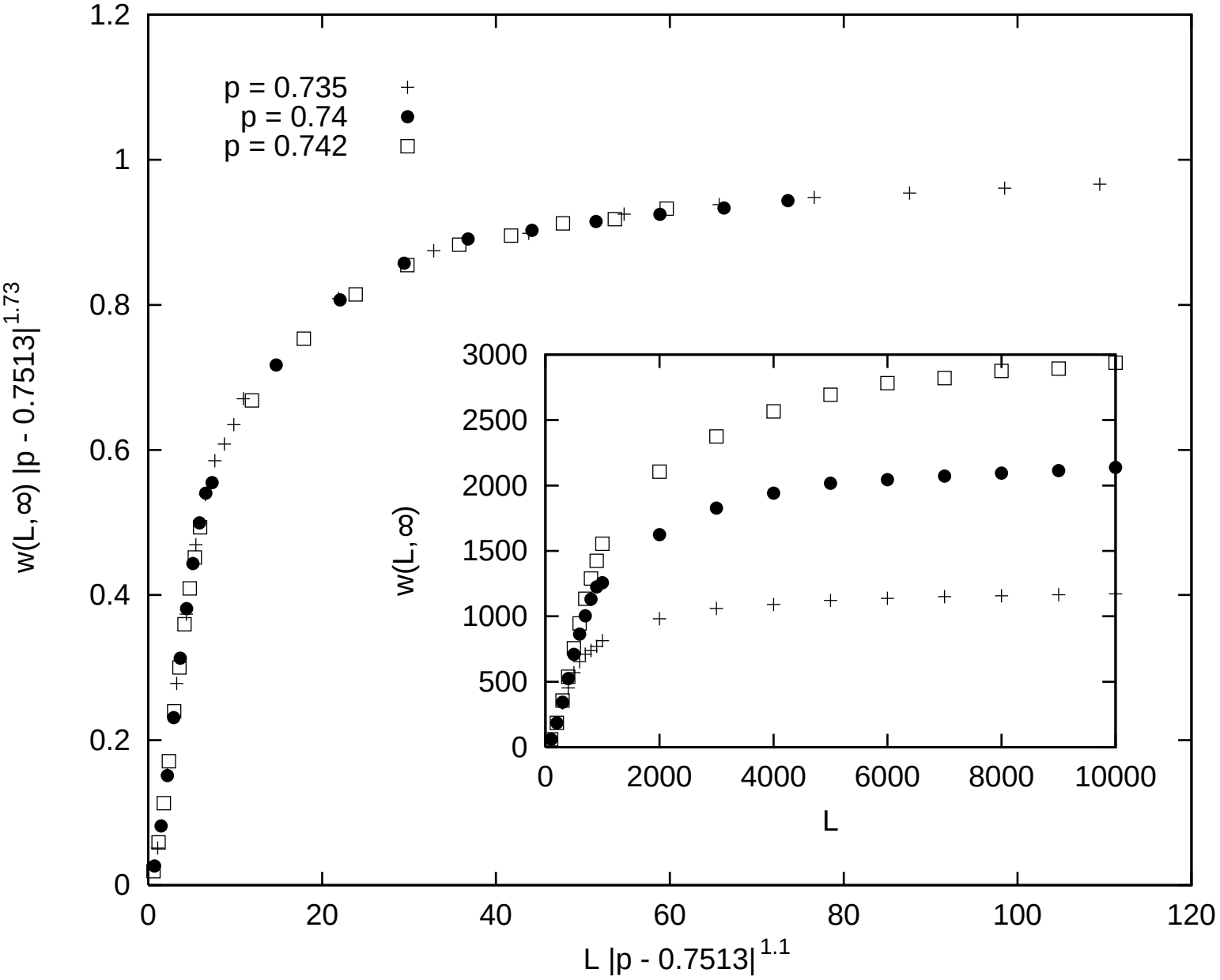
p = 0.735
p = 0.74
p = 0.742
w(L,∞) |p - 0.7513|^1.73
L |p - 0.7513|^1.1
w(L,∞)
L
0
20
40
60
80
100
120
0.2
0.4
0.6
0.8
1
1.2
500
1000
1500
2000
2500
3000
2000
4000
6000
8000
10000

Figure 3(b)

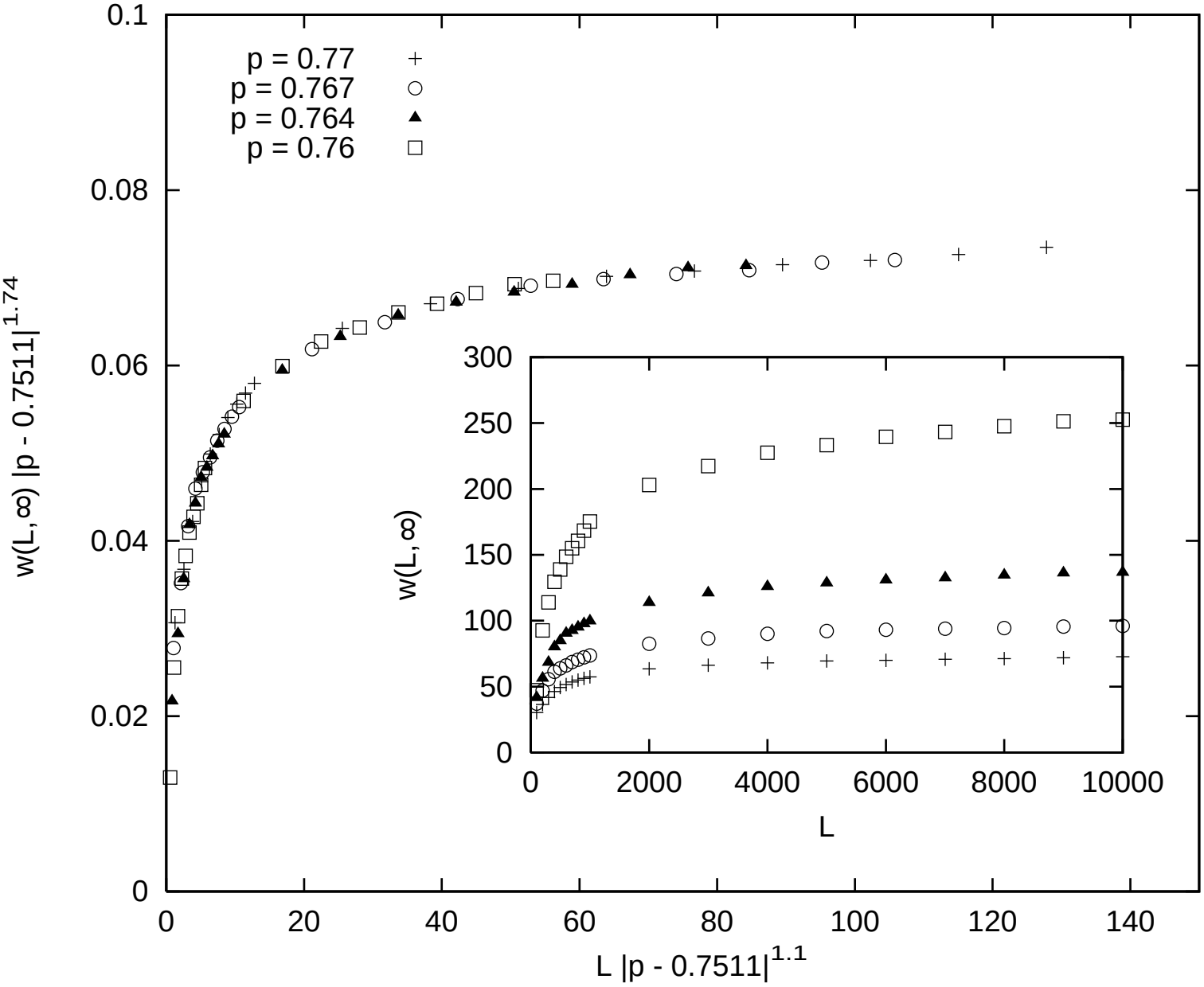
p = 0.77
p = 0.767
p = 0.764
p = 0.76
w(L,∞) |p - 0.7511|^1.74
L |p - 0.7511|^1.1
w(L, ∞)
L
0
0.02
0.04
0.06
0.08
0.1
0
20
40
60
80
100
120
140
0
50
100
150
200
250
300
0
2000
4000
6000
8000
10000

Figure 4

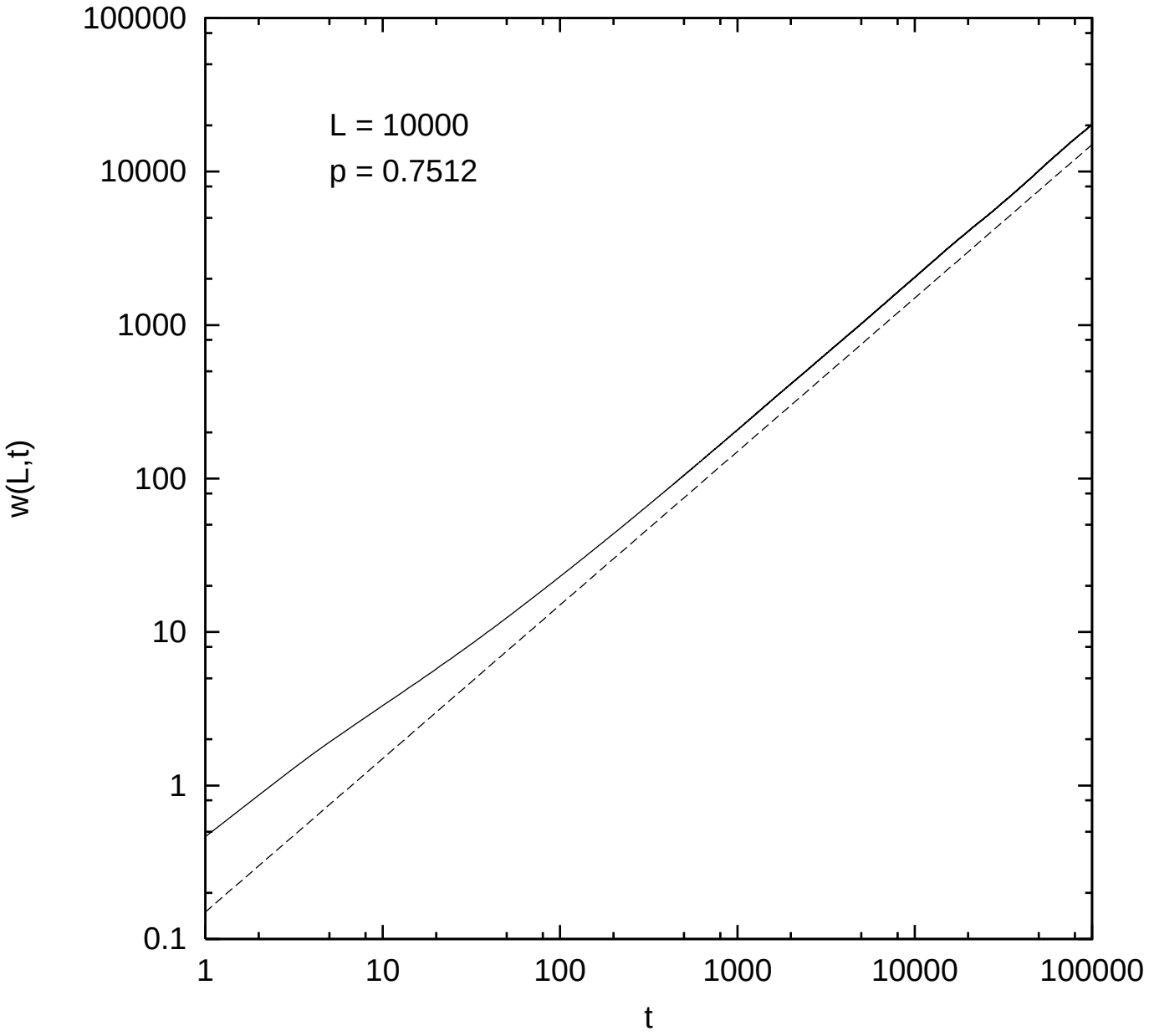
L = 10000
p = 0.7512
w(L,t)
t
100000
10000
1000
100
10
1
0.1
1
10
100
1000
10000
100000

Figure 5

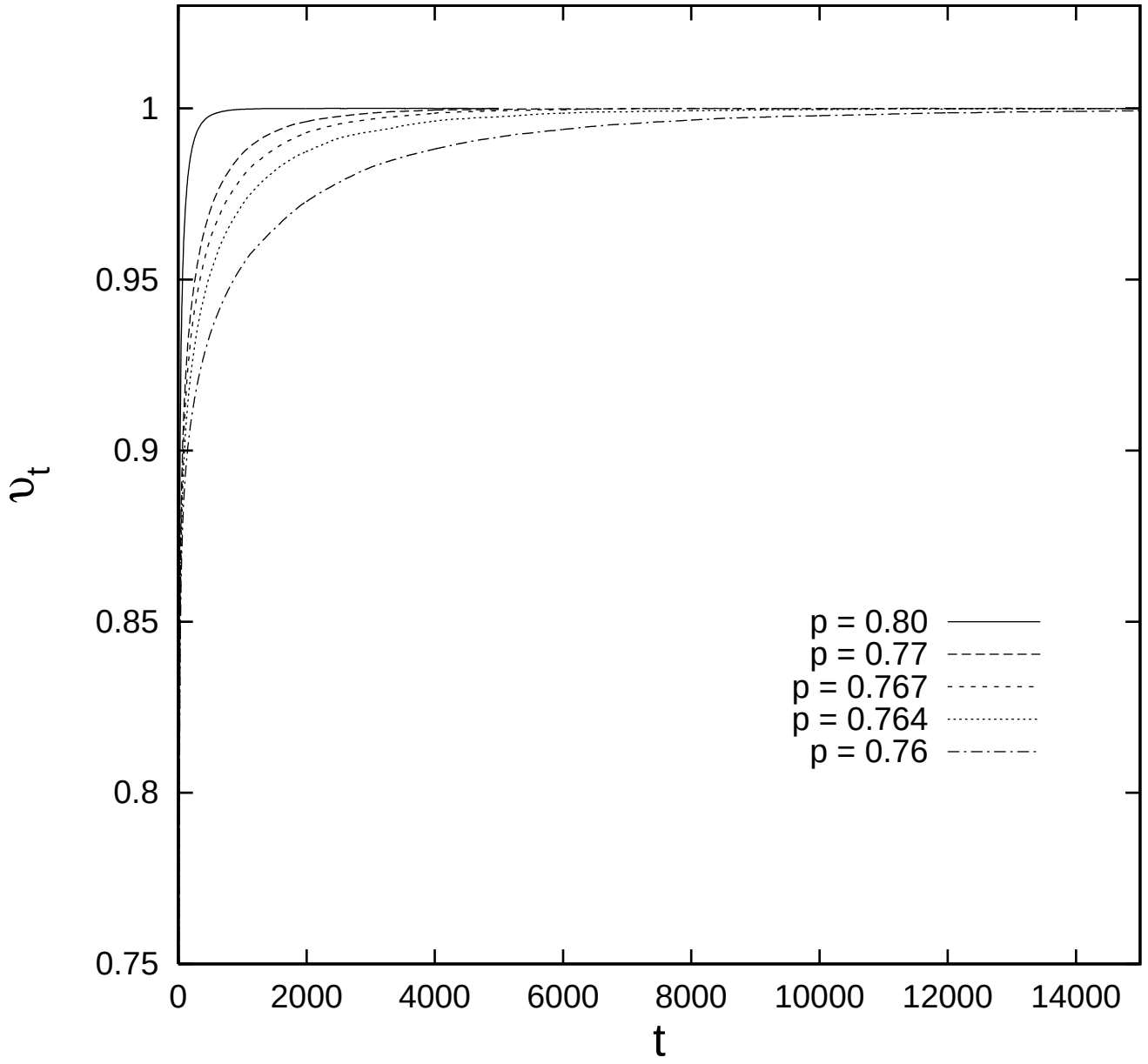
1
0.95
0.9
0.85
0.8
0.75
υ_t
0
2000
4000
6000
8000
10000
12000
14000
t
p = 0.80
p = 0.77
p = 0.767
p = 0.764
p = 0.76

Figure 6(a)

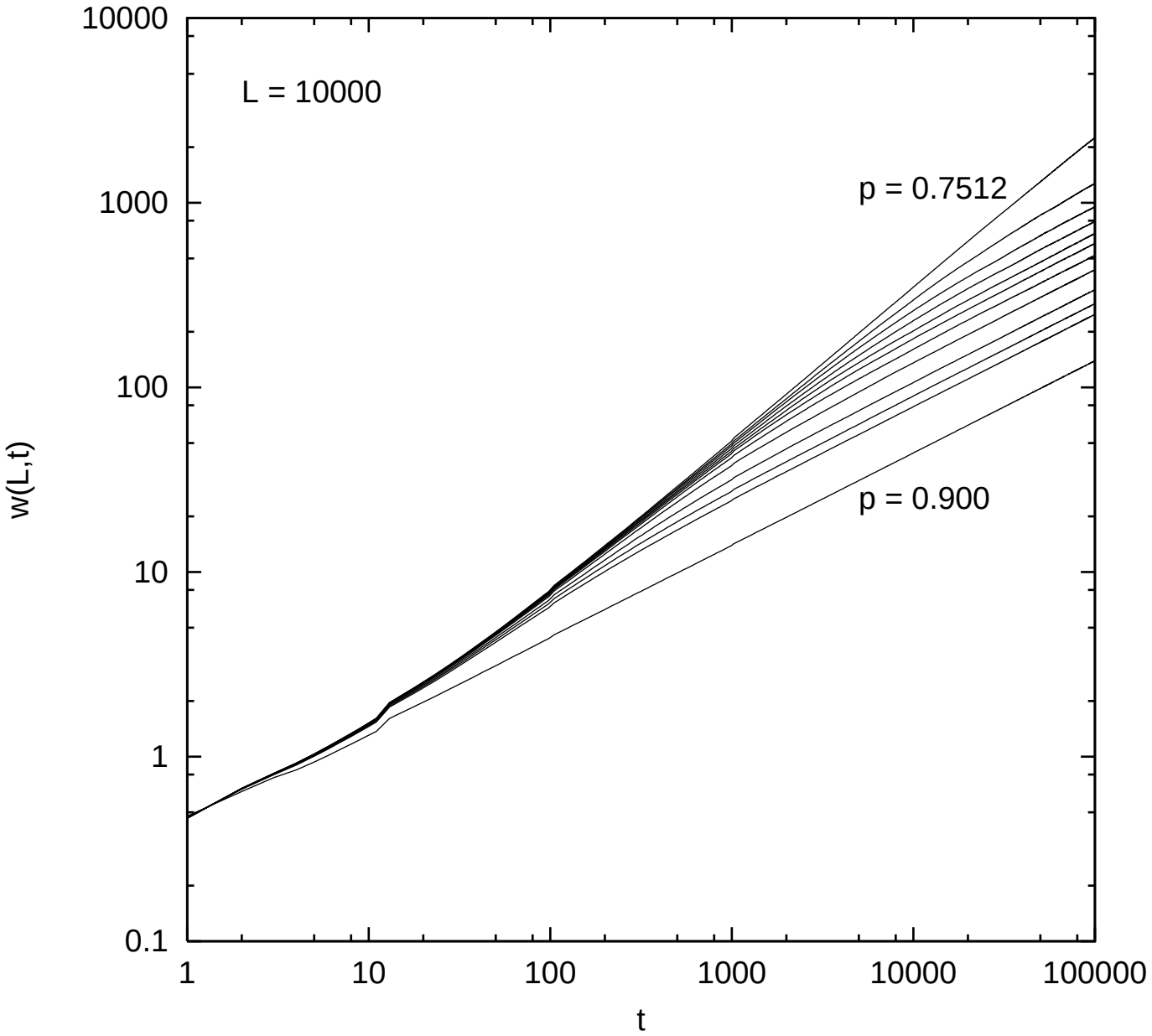
10000
1000
100
10
1
0.1
w(L,t)
L = 10000
p = 0.7512
p = 0.900
1
10
100
1000
10000
100000
t

Figure 6(b)

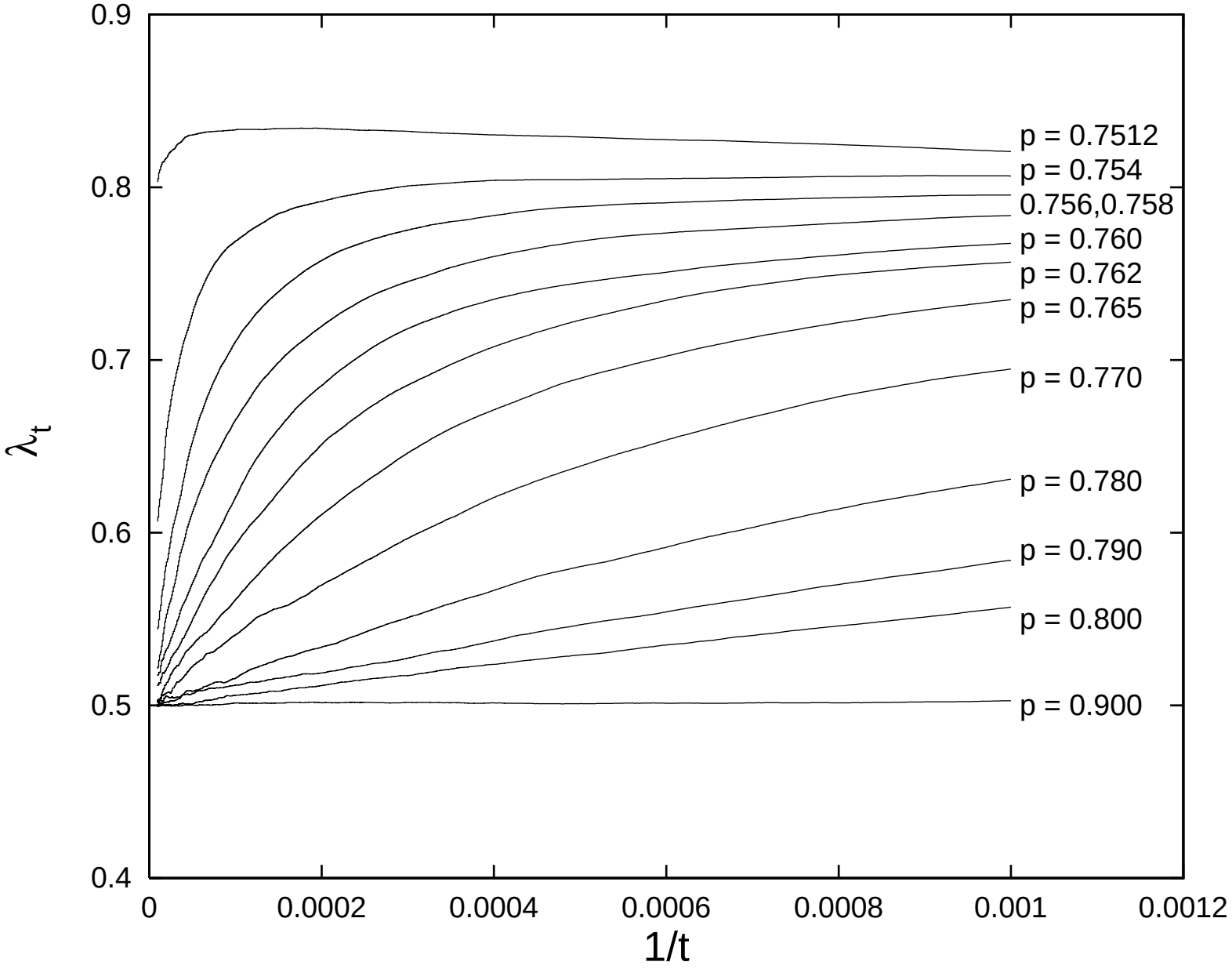
0.9
0.8
0.7
0.6
0.5
0.4
λ_t
0
0.0002
0.0004
0.0006
0.0008
0.001
0.0012
1/t
p = 0.7512
p = 0.754
0.756,0.758
p = 0.760
p = 0.762
p = 0.765
p = 0.770
p = 0.780
p = 0.790
p = 0.800
p = 0.900

Figure 7

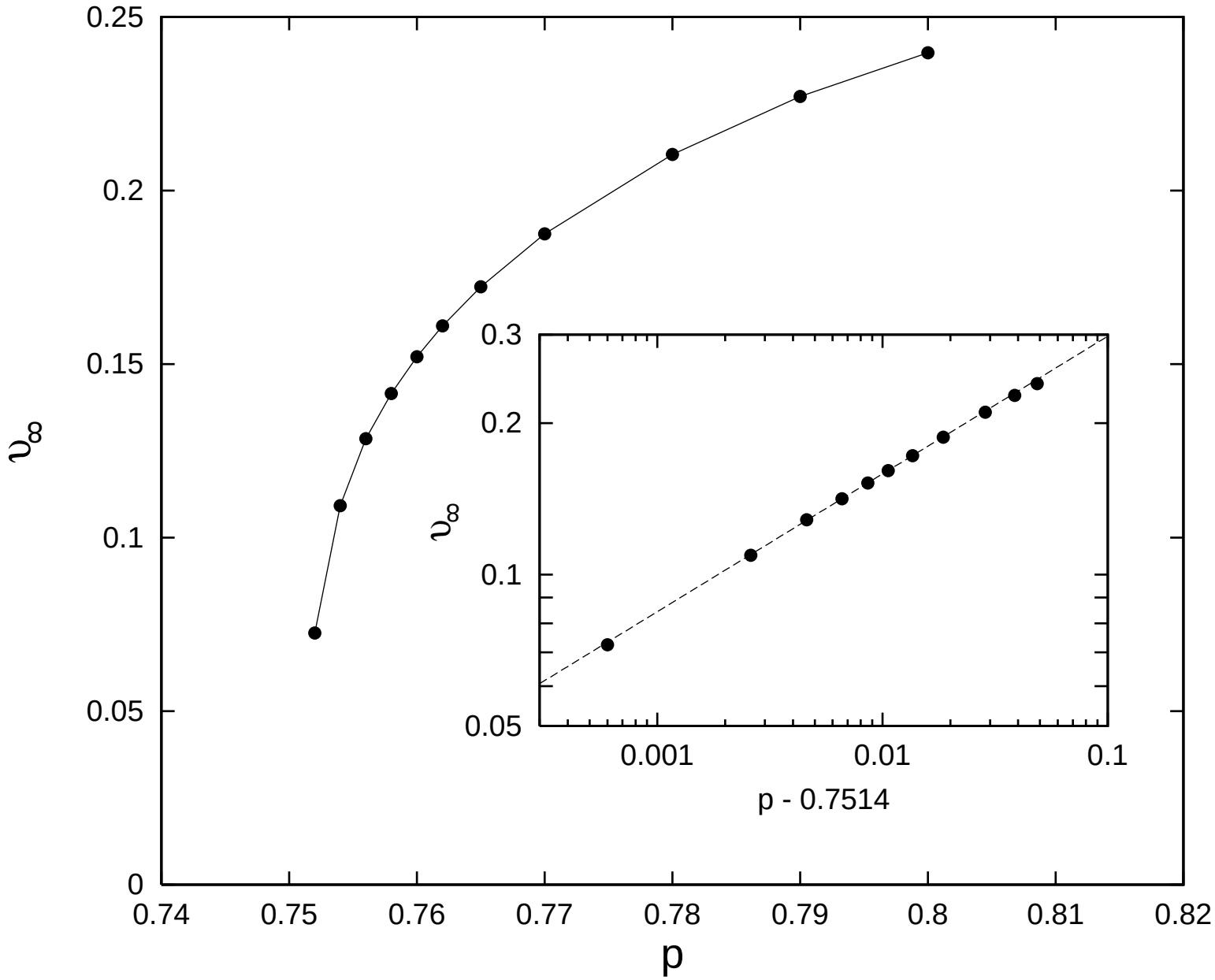
0.25
0.2
0.15
0.1
0.05
0
υ_8
0.74
0.75
0.76
0.77
0.78
0.79
0.8
0.81
0.82
p
0.3
0.2
0.1
0.05
υ_8
0.001
0.01
0.1
p - 0.7514